Short communication

BCY-based proton conducting ceramic cell: 1000 h of long term testing in fuel cell application

J. Dailly*, M. Marrony

European Institute For Energy Research (EIFER), Emmy-Noether-Str 11, 76131 Karlsruhe, Germany

HIGHLIGHTS

- All samples were prepared using commercial powders.
- 1000 h of long-term measurement without electrical degradation have been validated.
- No electrical degradation is observed on the voltage even after dynamic load cycles.
- No real chemical reactivity/decomposition or interface/material degradation occurred.

ARTICLE INFO

ABSTRACT

A Protonic Ceramic Fuel Cell based on commercial powder has been made by wet chemical routes. The $NiO-BaCe_{0.9}Y_{0.1}O_{3-\delta}$ substrate was initially elaborated by tape-casting, pre-sintered then a $BaCe_{0.9}Y_{0.1}O_{3-\delta}$ electrolyte was deposited by screen printing method. The whole half-cell is co-fired then $Nd_2NiO_{4+\delta}$ cathode is coated by screen-printing onto half-cells. A high and stable open circuit voltage was measured at the operating temperature of 600 °C (OCV = 1.06 V), indicating excellent gas-tightness of the protonic ceramic membrane. Although, the single cell shows modest power density of 60 mW cm^{-2}, for the first time, nearly 1000 h at 600 °C have been successfully operated without any loss voltage. Post-test analysis didn't evidence any delamination, reactivity or decomposition of any layer, meaning a good chemical stability of selected materials during fuel cell operation.

© 2013 Elsevier B.V. All rights reserved.

1. Introduction

Protonic Ceramic Cells gain recently interest in fuel cell application regarding their intrinsic advantages, more especially the non-dilution of the fuel at the anode side and the limited ageing of materials linked to the moderate operation temperature domain (400–600 °C).

Thus, many studies were done to improve the conductivity and the stability of protonic electrolytes [1–4], as well as finding new electrode materials in order to get better interfaces electrodes/electrolyte [5–8].

Among the wide variety of proton conductors, barium cerates present the highest protonic conductivity in the temperature range of 400–700 °C, especially the yttrium doped-one commonly noted BCY [9–13]. A theoretical thermodynamic instability of Ba containing oxides towards atmospheres containing carbon dioxide has been reported and mainly demonstrated on powder material or on sintered samples under severe conditions [14–16]. In fact, no link between real fuel cell testing conditions and accelerating ageing processes has been established until now.

PCFC performances up to 400 mW cm^{-2} have been registered in the literature. But in most cases, the electrolyte/anode half-cell was made by co-pressing method, which is not suitable at industrial scale [17]. Moreover, the active area is generally below than 1 cm^2 [18,19]. Finally, only few publications report endurance test measurements under OCV or galvanostatic profile and exposed in general less than few tens hours [17,20–23].

In this study, protonic ceramic cells based on a yttrium-doped barium cerate electrolyte and a mixed-conductor type neodymium nickelate cathode has been elaborated by compatible industrial wet chemical routes. Both tape-casting and screen-printing processes are used. *Ante-test* and *post-test* physical analysis are then

* Corresponding author. Tel.: +49 721 6105 1352; fax: +49 721 6105 1332.
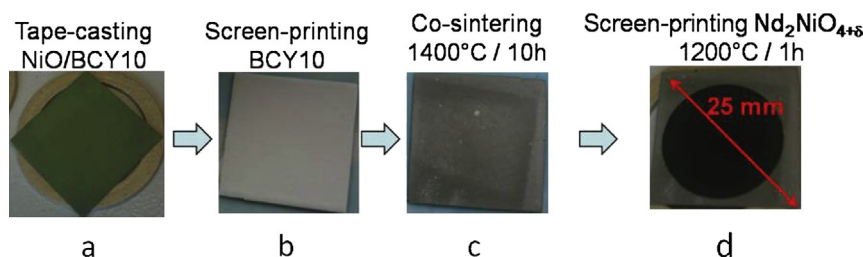 *E-mail address:* dailly@eifer.org (J. Dailly).

Fig. 1. Elaboration process of the cell.

used to highlight the quality level of the microstructure and the chemical stability of cell layers. Finally, optimized testing conditions are described and current–voltage characteristics of homemade BCY-based cell are assessed under a long-term galvanostatic measurement at 600 °C.

2. Experimental

2.1. Powders

All samples were prepared using commercial powders (supplier Marion Technologie®), listed below:

- Hydrogen electrode: $NiO-BaCe_{0.9}Y_{0.1}O_{3-\delta}$ (60 wt.%/40 wt.%),
- Electrolyte: $BaCe_{0.9}Y_{0.1}O_{3-\delta}$
- Air electrode: $Nd_2NiO_{4+\delta}$

A combustion process has been used to promote grain sizes reduced. It involves metal salts with an oxidant (nitric acid, urea, glycine). The initiation of the reaction takes place at 800 °C and lead to the formation of the desired oxide, but a heat treatment is necessary to obtain a pure phase (for instance 1400 °C for $BaCe_{0.9}Y_{0.1}O_{3-\delta}$ and $NiO-BaCe_{0.9}Y_{0.1}O_{3-\delta}$) [17].

2.2. Preparation of the anode substrate by tape-casting

The hydrogen electrode-support has been made by tape-casting. The anode slurry was prepared by mixing in a Turbula® type T2F (WAB) the $NiO-BaCe_{0.9}Y_{0.1}O_{3-\delta}$ powder in mixed solvent (MEK/ethanol) with the addition of a dispersing agent for 24 h. The binder and plasticizers were added and further milled for 3 h before a standing period of 48 h. Then, the slurry was de-aired for 15 min before casting.

The slurry was cast on a glass support coated with polymer thin film to prevent adhesion of the green tapes. A 500 μm thick anode layer was cast and left for one day at room temperature. Sample squares were cut into the dried green tape and pre-sintered at 1000 °C during 4 h (cf. Fig. 1a).

2.3. Preparation of the electrolyte layer by screen-printing

Fine $BaCe_{0.9}Y_{0.1}O_{3-\delta}$ powder was used as precursors. The primary paste was prepared by dissolving 6 wt.% ethyl–cellulose into

terpineol. 50 wt.% electrolyte powders were subsequently added into the primary paste, then milled and homogenized together using a three roll mill during 30 min.

Ceramic membrane of $BaCe_{0.9}Y_{0.1}O_{3-\delta}$ was deposited on the pre-sintered anode-substrate by a screen-printing method. The coated substrate was then dried in a ventilated drying-box during 10 min and then re-printed (cf. Fig. 1b). After drying, the coated layer was fired in air at 1350 °C during 9 h (heating rate was 1 °C min^{-1}). Then, two firing steps were needed in order to obtain flat half-cells (1300 °C during 2 h under alumina weight, respectively 80 and 400 g) (cf. Figs. 1c and 2).

2.4. Preparation of the air electrode layer by screen-printing

Fine $Nd_2NiO_{4+\delta}$ powder was mixed thoroughly in a three rolls mill together with a 6 wt.% ethylcellulose-terpineol binder to form the cathode slurry.

$Nd_2NiO_{4+\delta}$ layer was printed on the flat half-cell by the screen-printing technique. The coated half-cell was dried in a ventilated drying-box during 10 min and then printed again. After drying, the coated substrate was fired in air at 1100 °C during 3 h. The heating rate was 1 °C min^{-1} from room temperature to 400 °C and 3 °C min^{-1} above 400 °C (cf. Fig. 1d). The obtained sample was a 3.6 cm^2 square (35 × 35 mm) with a round active area of 2.01 cm^2. The cell morphologies are observed before and after electrochemical characterizations by field-emission scanning electron microscopy.

2.5. Test procedure and operating conditions

Electrical contacts to the cell were made using platinum wires welded to the Pt meshes used as current collectors. Pt meshes are
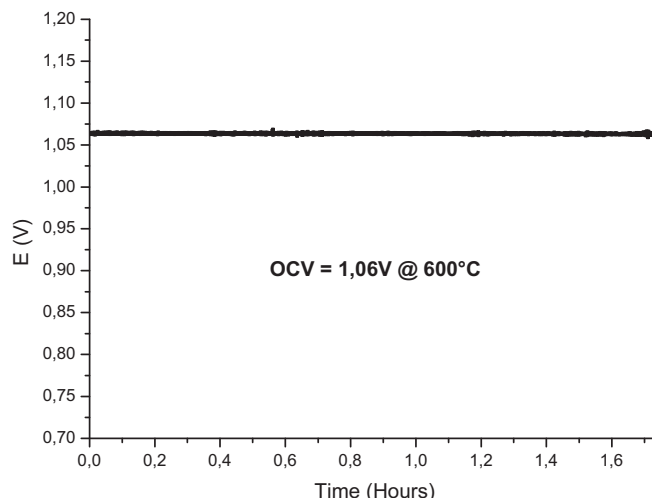

Fig. 2. First ironing step.

OCV = 1,06V @ 600°C

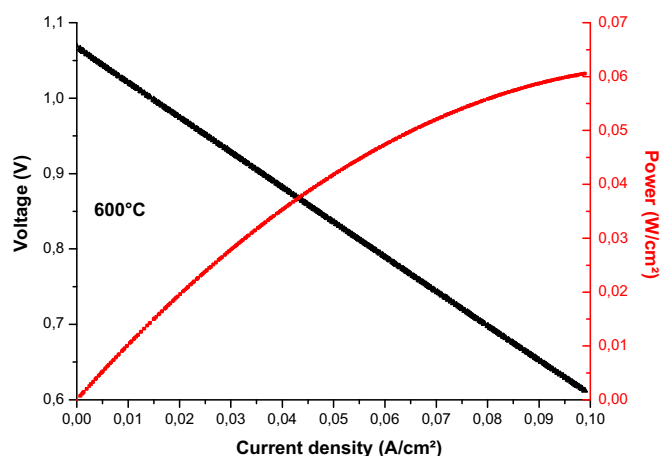**Fig. 3.** OCV measurement during 1 ½ hours.

Fig. 4. Performance of the as-prepared cell at 600 °C.

placed on alumina supports which aim at diffusing the corresponding gas. Even if this configuration is not completely sealed (which means that some fuel burns at the periphery of the cell), Thermiculite 866 gaskets provided by Flexitallic® has been used to absorb the mechanical pressure on the cell and to avoid any contact between ceramic tubes from test bench and the cell. The gas flows were controlled by Brooks mass flow controllers and current/potential data were collected by a Solartron 1286.

During the heating ramp (speed = 1 °C min^{-1}) up to 600 °C (operating temperature), flow rates were 70 mL min^{-1} at both electrodes (air at the cathode side and nitrogen at the anode side). The nickel oxide was then reduced in 100% Hydrogen. The experiment was performed under non-humidified ambient air and gas-bottle hydrogen.

3. Results and discussion

3.1. Fuel cell mode

As shown in Fig. 3, the high Open Circuit Voltage of 1.06 V ± 1 mV at 600 °C indicates not only the electrolyte membrane is dense enough but also shows BCY10 is a pure ionic conductor at 600 °C. The OCV remains very stable during more than 1 ½ h.
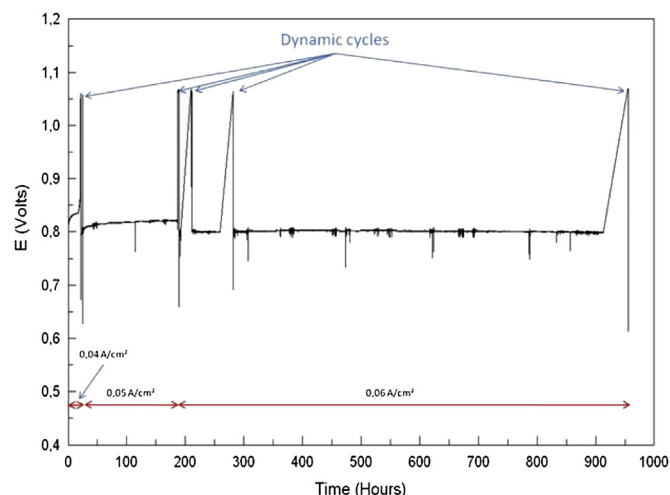

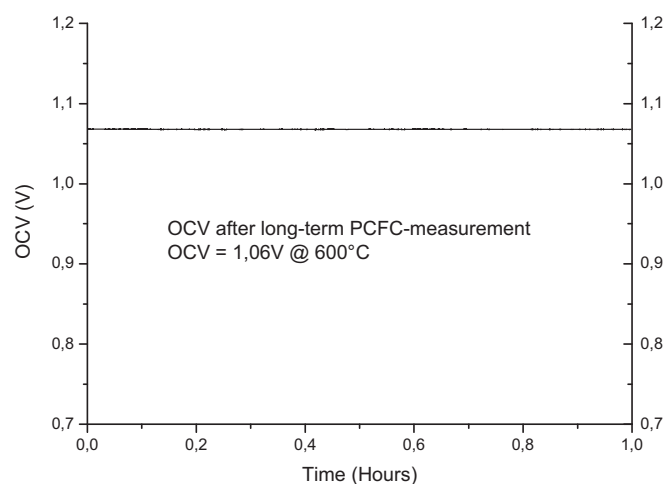Fig. 5. Long term measurement under galvanostatic conditions.

Fig. 6. OCV stability after PCFC long-term measurement.

Fig. 4 presents the current–voltage characteristic (I–V) and power density (I–P) of the as-prepared cell at 600 °C. The almost linear I–V curve implies low electrode polarization resistance and small charge transfer activation effect. The total Area Specific Resistance of the cell was calculated from the slop of the I–V curve (ASR$_{cell}$ = 4.8 Ω cm^{-2} at 600 °C) and is comparable to previous results reported by Taillades et al. with Pr$_2$NiO$_{4+\delta}$/BCY10/BCY10-Ni cell [21]. A power density value higher than 60 mW cm^{-2} is measured at 600 °C. It is well know that, among nickelates compounds, the neodymium phase exhibits the highest chemical stability but lower electrochemical performances than the praseodymium one. That's partially explains the relative low value of maximal power density measured.

Long-term measurement (950 h) has been performed under galvanostatic conditions (Fig. 5). Three main domains are observed, corresponding to three current conditions (40, 50 and 60 mA cm^{-2}).

During the first hours, the electrical contact has been improved by applying a pressure on platinum grid, which leads to a significant increase in voltage. The current was then increased to 50 mA cm^{-2} and a slight augmentation of the voltage was again observed. This phenomenon can be attributed to the slow kinetic of reduction of the nickel, caused by the dense morphology of the anode substrate (see "Microscopic Analysis" paragraph). Finally, a
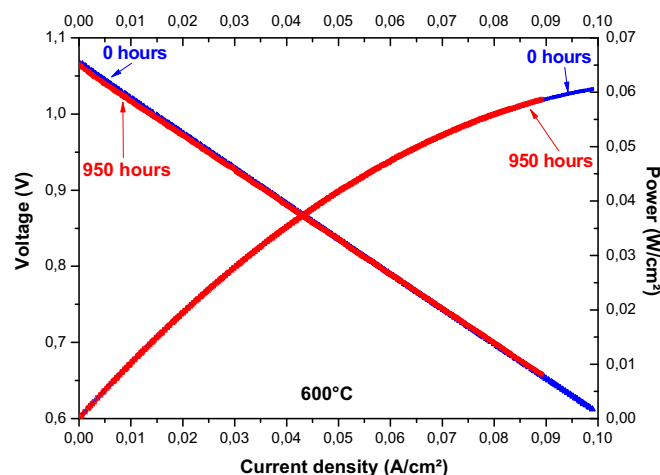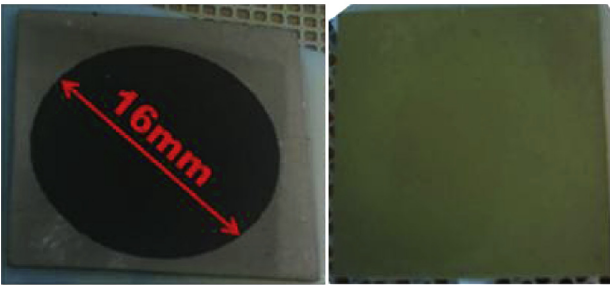

Fig. 7. Comparison of I–V characteristics at 0 h and 950 h.

Before Electrochemical measurements

After Electrochemical measurements

Fig. 8. Macroscopic views of the cathode and anode sides before and after electrochemical measurements.

Table 1
Characteristics of each layer before and after electrochemical measurements.

	Thickness		Porosity	
	Before	After	Before	After
Cathode	17 µm	16 µm	29%	27%
Electrolyte	27 µm	25 µm	4%	6%
Anode	430 µm	430 µm	5%	18%

1000 h and under polarization at 600 °C would show no real chemical reactivity/decomposition or interface/material degradation occurred under oxidant (cathode) and reduced (anode) atmospheres.

3.2. Macroscopic analysis

Fig. 8 shows macroscopic views of the cell before and after electrochemical measurements. The various prints on the surface of both electrodes correspond to gas channels from ceramic support. From a macroscopic point of view, nickel seems to be fully reduced by the grey colour observed of the anode substrate (NiO is green whereas Ni-metallic is grey). On the other side, there is no visual delamination of the air-electrode, the cathode material being well stuck on the electrolyte. Finally, no crack or failures have been observed which certifies a good mechanical integrity of the cell.

3.3. Microscopic analysis

Fig. 9 presents cross section images of the half-cell assembly *ante-* (a) and *post-test* (b). Both samples are very planar and crack-free. The anode is 430 µm thick (Table 1); NiO and BCY10 phases seem to be homogeneously distributed and no nickel segregation is observed after test. The anode porosity is nearly 5% at the beginning and increases up to 18% (calculated by image software analysis ImageJ©): this phenomenon is attributed to the reduction of nickel oxide into metallic nickel. To note, the low value of porosity at the beginning can explain the slow reduction observed during the test.

It can also be seen that both electrodes adhered very well to the membrane, even after 1000 h under polarization. Beside, although the electrolyte seems to be more porous, especially at the cathode side; no real decomposition of the barium cerate as well as chemical reactivity is evidenced. However, further investigation has to be done to clarify this observation.

Finally, no delamination at the cathode/electrolyte interface is observed, and the microstructure of the nickelate phase remains homogeneous and enough porous after ageing.
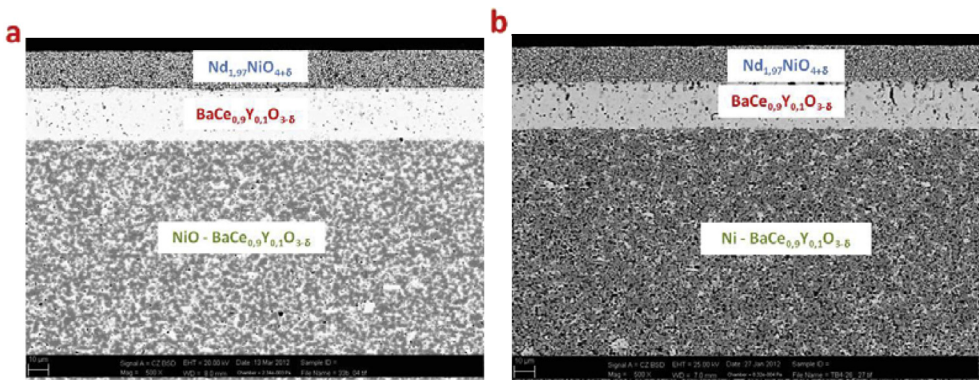
current density corresponding to a potential of 0.8 V has been applied ($i = 60$ mA cm^{-2}).

The single cell voltage remains stable with constant discharge current of 60 mA cm^{-2} during nearly 1000 h, corresponding to a power density of 50 mW cm^{-2}. Moreover, no electrical degradation is observed on the voltage even after dynamic load cycles realized between OCV and 0.8 V (corresponding to current shutdown issues, I−V curves).

OCV stability was checked during 1 h after the long-term measurement. The picture 6 shows that the open circuit voltage remains stable after 1000 h of operation (OCV = 1.06 V ± 1 mV) (cf. Fig. 3) (Fig. 6).

Finally, current−voltage characteristics have been compared after and before galvanostatic measurement (Fig. 7). According to the stable voltage observed previously, the electrical performance of the cell remains the same before and after long-term polarization. The great electrical stability of the sample exhibited during

Fig. 9. SEM micrographs of cell (a) before and (b) after testing.

4. Conclusion

A complete anode supported proton conducting cell (PCC) has been made in EIFER laboratory, where facilities concerning powder synthesis and cell manufacturing have been recently improved. 35×35 mm cells have been manufactured by wet chemical routes (tape casting for the Ni–BCY10 anode; screen-printing for the BCY10 electrolyte; screen-printing for the $Nd_2NiO_{4+\delta}$ cathode) and electrochemical tests have been performed.

Although modest power density was obtained (60 mW cm^{-2} at 600 °C) with an area specific resistance of 4.9 Ω cm^2, 1000 h of long-term measurement without electrical degradation have been validated, corresponding to our knowledge of the best results raised in the Proton conducting ceramic cell domain research. Microstructure of the cell before and after electrochemical test was investigated by SEM analysis and revealed planar and crack-free assemblies. The 30 μm electrolyte layer is well densified whereas the porosity of the substrate remains to improve. Further works have to be considered in order to optimize the structure of the whole PCC system (substrate porosity, electrolyte thickness, composition and architecture of the air electrode, interlayer nature, etc…), and those for improving performances while keeping long-term stability properties.

Acknowledgement

References

[1] Z. Khani, M. Taillades-Jacquin, G. Taillades, M. Marrony, D.J. Jones, J. Rozière, J. Solid State Chem. 182 (2009) 790–798.
[2] H. Ding, Y. Xie, X. Xue, J. Power Sources 196 (2011) 2602–2607.
[3] M. Wang, L. Qiu, X. Cao, J. Rare Earths 29 (2011) 678–682.
[4] P. Pasierb, M. Osiadły, S. Komornicki, M. Rekas, J. Power Sources 196 (2011) 6205–6209.
[5] J. Dailly, S. Fourcade, A. Largeteau, F. Mauvy, J.C. Grenier, M. Marrony, Electrochem. Acta 55 (2010) 5847–5853.
[6] H. Wang, Z. Tao, W. Liu, Ceram. Int. 38 (2012) 1737–1740.
[7] J. Dailly, F. Mauvy, M. Marrony, M. Pouchard, J.-C. Grenier, J. Solid State Electrochem. 15 (2011) 245–251.
[8] L. Yang, S. Wang, X. Lou, M. Liu, Int. J. Hydrogen Energy 36 (2011) 2266–2270.
[9] T. Hibino, A. Hashimoto, M. Suzuki, M. Sano, J. Electrochem. Soc. 149 (2002) A1503–A1508.
[10] Z.-T. Tao, Z.-W. Zhu, H.-Q. Wang, W. Liu, J. Power Sources 195 (2010) 3481–3484.
[11] X.-Z. Fu, J.-L. Luo, A.-R. Sanger, N. Luo, K.-T. Chuang, J. Power Sources 195 (2010) 2659–2663.
[12] W. Suksamai, I.-S. Metcalfe, Solid State Ionics 178 (2007) 627–634.
[13] T. Shimura, H. Tanaka, H. Matsumoto, T. Yogo, Solid State Ionics 176 (2005) 2945–2950.
[14] K. Katahira, Y. Kohchi, T. Shimura, H. Iwahara, Solid State Ionics 138 (2000) 91–98.
[15] J.-H. Kim, Y.-M. Kang, M.-S. Byun, K.-T. Hwang, Thin Solid Films 520 (2011) 1015–1021.
[16] N. Zakowsky, S. Williamson, J.T.S. Irvine, Solid State Ionics 176 (2005) 3019–3026.
[17] M. Marrony, Proton conducting ceramic cells: status and prospects, in: Oral Communication, SSPC16 Conference 10–14.09.2012, Grenoble (France), 2012.
[18] Y. Guo, Ran Ran, Z. Shao, Int. J. Hydrogen Energy 36 (2011) 1683–1691.
[19] W. Sun, Y. Jiang, Y. Wang, S. Fang, Z. Zhu, W. Liu, J. Power Sources 196 (2011) 62–68.
[20] J. Dailly, Ph.D. thesis, Université de Bordeaux, France, 2008.
[21] G. Taillades, J. Dailly, M. Taillades-Jacquin, F. Mauvy, A. Essouhmi, M. Marrony, C. Lalanne, S. Fourcade, D.J. Jones, J.-C. Grenier, J. Rozière, Fuel Cells 10 (2010) 166–173.
[22] L. Zhao, B. He, Y. ling, Z. Xun, R. Peng, G. Meng, X. Liu, Int. J. Hydrogen Energy 35 (2010) 3769–3774.
[23] L. Bi, S. Zhang, L. Zhang, Z. Tao, H. Wang, W. Liu, Int. J. Hydrogen Energy 34 (2009) 2421–2425.